

INTERNAL REPORT SDL-94-\*\*  
01/02

**SUMMARY OF SHOCK EXPERIMENTS ON SILICON CARBIDE  
UP TO 250 KBAR**

G. F. Raiser, R. Feng, and Y. M. Gupta

October 1994

Shock Dynamics Laboratory

Dept. of Physics

Washington State University

Pullman, WA 99164

## I. Introduction

A series of experiments has been performed on "PAD" (pressure-assisted densification) SiC type B from Cercom Inc. of Vista, California. The overall objective of this ongoing project is to achieve a clear understanding of both how a ceramic material responds to high stresses/loading rates and the micromechanical processes determining its behavior. As a first step, the current experiments were conducted with the goal of measuring the strength of SiC in the shocked state. In order to do this, SiC samples were impacted to stresses below and above the HEL (approximately 120 kbar) and response of longitudinal and lateral in-material piezoresistance gauges was monitored. Conversion of resistance change to stress is accomplished for the longitudinal gauges. Analysis of the lateral gauge output is more complicated [1]. The purpose of this report is to summarize the results as they stand at the moment in an easily updatable format. This document will serve as a reference for all of the piezoresistance gauge experiments conducted on SiC.

## II. Material and Experimental Description

The impactor material used for these experiments was OFHC copper, while the target specimens were made from different blocks of silicon carbide ( $\alpha$ -SiC, type 6H) from the supplier mentioned above. Table I is a summary of various material attributes of this ceramic. Density was measured using the Archimedes method, and sound speeds were obtained from the Army Research Laboratory (Watertown, MA). The elastic moduli were then calculated from these measurements.

The first experiment (shot 93-514) was conducted on the 2.5 inch diameter light-gas gun at WSU, while the 4 inch diameter gun was used for the remaining experiments. For velocities up to 0.8 mm/ $\mu$ sec, eight-inch aluminum projectiles were used, while six-inch projectiles were used for the higher velocities. Both types of projectiles were capped on the back. In all shots, an OFHC copper impactor plate was mounted on the impact face of the projectile. The impact configuration is shown in Figure 1 as well as specimen assemblies for the two cases of longitudinal and lateral gauge shots. In order to minimize wave interactions between multiple interfaces, several shots were designed with only one piezoresistance gauge inside the specimen. Resistances of the gauge leads and active elements were determined as described by Wong [1]. These target assemblies were then potted into a steel ring coplanar with the face of the ring along with coaxial cables for stand-off and surface triggers, and tilt measurement. The target assembly was then lapped to a final flatness and checked with a micrometer (flatness better than 0.0005" over the face of the specimen).

Cables were soldered to the gauges and connected to the gauge power supply (for the power leads) and Tektronix DSA 602A digital oscilloscopes (for the sensor leads). An ambient test was run using a delay generator to simulate the sequence of events during the actual experiment. The oscilloscopes were triggered manually through the stand-off and surface trigger cables and each individual tilt pin and the resultant records were stored onto floppy disks.

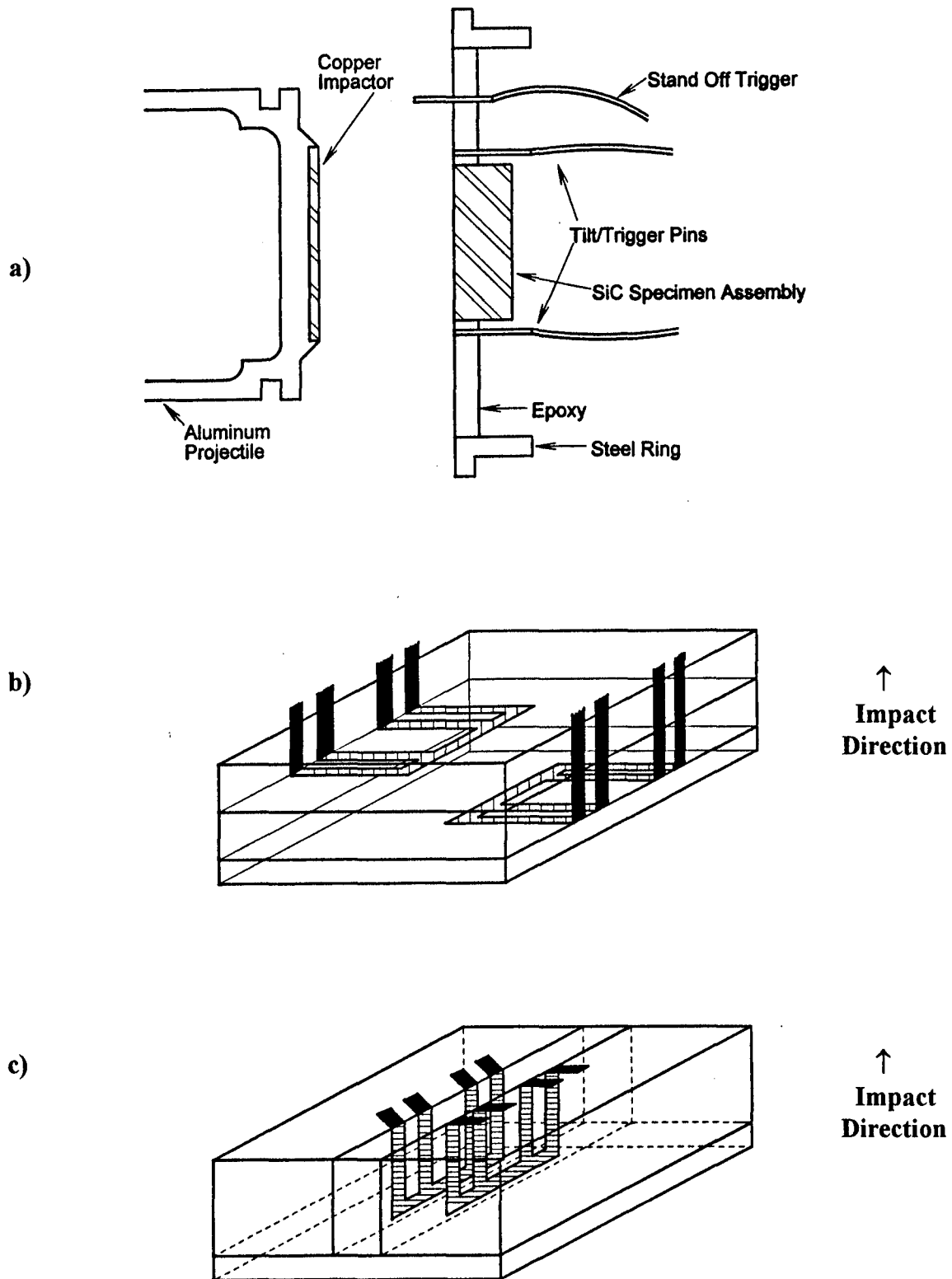


**Figure 1:** Schematics of a) the experimental impact configuration, b) the gauge placement for longitudinal gauge experiments, and c) the gauge placement for lateral gauge experiments.

The target holder was then aligned, a velocity measurement block was installed and the target was attached to the holder. After inserting the projectile into the breech end of the gun, closing the chamber and attaching the catcher tank, the gun was pumped down to approximately 50 mtorr and fired.

### III. Longitudinal Gauge Results

A summary of the longitudinal gauge experimental results is presented in Table II, and graphs of  $(\Delta R/R_o)$  vs. time for every longitudinal gauge experiment can be found in Appendix A. Premature failure of the first gauge in experiment 93-017 (and the resultant interference with the second gauge) prevented accurate recording of the voltage signal for the latter gauge. The last two columns in Table II contain the end-state longitudinal stress and corresponding particle velocity for each experiment. They were calculated as follows.

#### A. Calculation of Stresses - Gauge Calibration

First, a calibration relation was needed to convert peak resistance change to longitudinal stress according to the empirical formula:

$$\frac{\Delta R}{R_o} = K \cdot \sigma_n, \quad (3.1)$$

where in general,  $K = K(\sigma_n)$ . Surface-gauge measurements (as opposed to gauges in grooves) in known matrix materials of the configuration used for these tests are sparse. The available data from Brar and Gupta [2] and Wong [1] have been plotted in Figure 2 along with data from two symmetric impact experiments in OFHC copper. A quadratic fit to the data is also presented. The experimental calibration coefficient is determined, through least-squares fitting, to be  $K=2.995 \times 10^{-3} \text{ kbar}^{-1} - (1.850 \times 10^{-6} \text{ kbar}^{-2})\sigma_x$ . The longitudinal stresses for the two copper shots (at about 205 and 235 kbar) were calculated using Feng and Gupta's [3] relation between longitudinal stress and particle velocity, assuming the peak particle velocity to be half of the impact velocity. For now, the above value of  $K$  is used along with the peak resistance measurements to obtain the peak longitudinal stress.

#### B. Calculation of Particle Velocity

The compressive peak state in these experiments can be represented in  $\sigma_x - u_p$  space as the intersection between the SiC and the OFHC copper Hugoniot curves. Although the SiC Hugoniot curve is not known, the peak stress in the SiC for any given experiment is known from Section A. The copper curve is constructed using the impact velocity, and the particle velocity at the point in that curve which corresponds to the peak stress is then the particle velocity of the peak state. In this way, particle velocities for each longitudinal gauge shot is determined. The OFHC copper Hugoniot is taken from Feng and Gupta [3]. The resultant  $\sigma_x - u_p$  points for SiC are plotted in Figure 3. The data is presented along

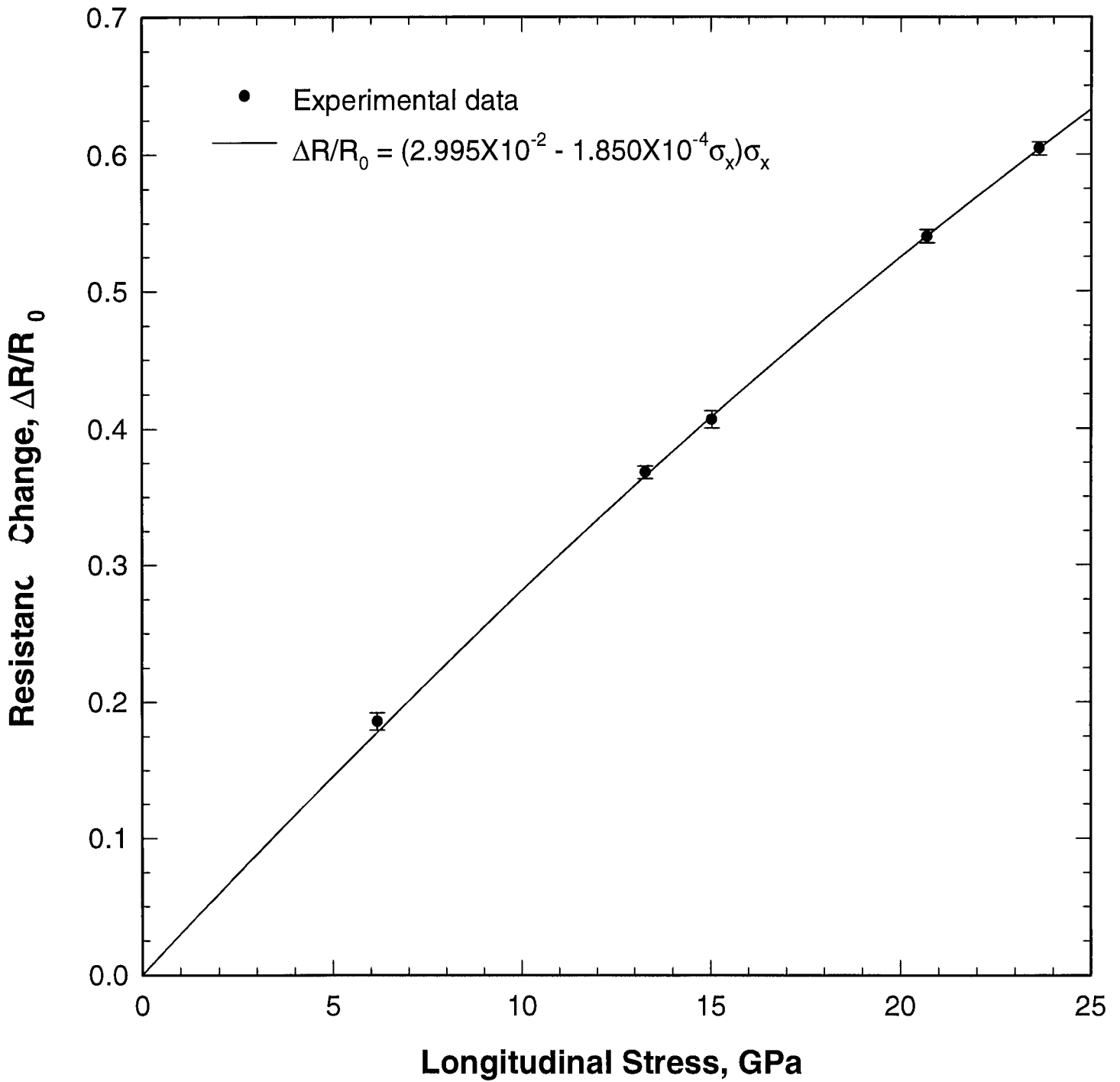


**Figure 2:** Results of longitudinal surface gauge experiments and the quadratic calibration relation used for conversion of peak resistance change to longitudinal stress.

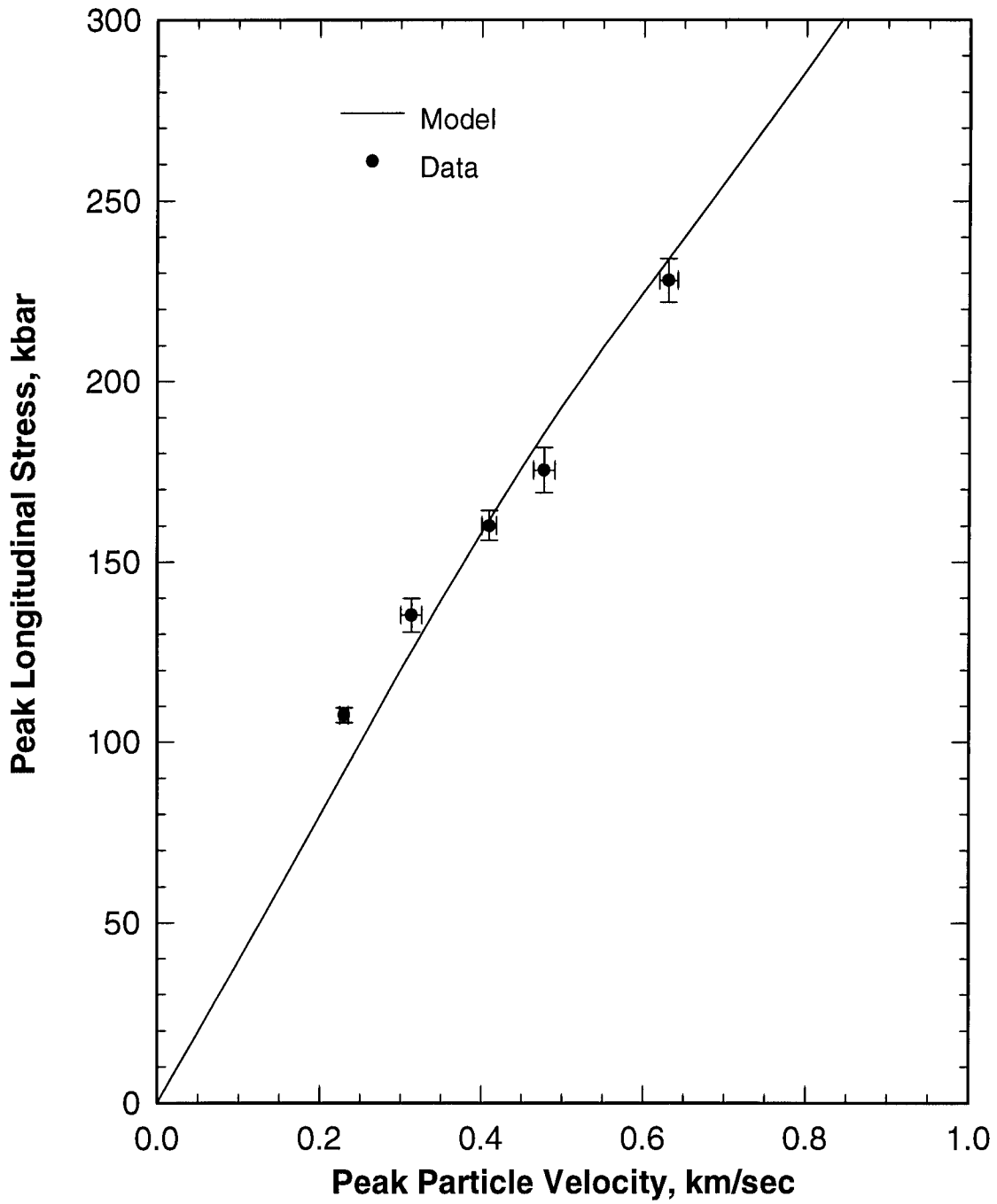


**Figure 3:** Results of longitudinal gauge experiments, plotted as Hugoniot data in  $\sigma_x - u_p$  space. Also plotted is the model fit to all available data on this SiC material.

with the material model developed by Feng *et al.* [4]. Grady and Crawford [5] estimate the HEL of this SiC to be about 117 kbar, which is the value used in the model.

### C. Note on Calculating Volume Compression

Ideally, one would like to establish the peak strain or, the compression  $\mu = V_0/V - 1$ , for each longitudinal gauge experiment. For steady or discontinuous waves, the jump conditions may be applied to calculate  $\mu$ . These experiments do not show clear discontinuities in the wave profiles. Likewise, there is no evidence to suggest that the compressive wave profile reached steady-state prior to arrival at any gauge location. Attempts to apply jump conditions on the assumption of two shock discontinuities results in very large errors. Determination of  $\mu$  has been done using the material modeling procedure [4].

## IV. Lateral Gauge Results

A summary of the lateral gauge experimental results is presented in Table III, and graphs of  $\Delta R/R_0$  vs. time for every lateral gauge experiment can be found in Appendix B. In one of the shots (93-070), grooves were machined into the SiC specimen and the gauges were embedded in these grooves. This configuration is meant to experimentally approximate the condition of an elastic-plastic inclusion in an elastic matrix that was analyzed by Gupta and Gupta [6]. The gauge resistance change for this shot was slightly lower than the surface gauge results, but not significantly. The last two columns in Table III contain the end-state longitudinal stress and corresponding particle velocity for each experiment. They were calculated as follows.

### A. Calculation of Longitudinal Stresses and Particle Velocities

Since these experiments did not contain longitudinal gauges, the peak stresses and particle velocities were determined by calculating the intersection in  $\sigma_x - u_p$  space of the OFHC copper Hugoniot and the modeled SiC Hugoniot curve [4], given the impact velocity. Uncertainties in the impact velocity were accounted for in the error estimation (see Section V).

### B. Combined Longitudinal and Lateral Gauge Results

Figure 4 is a plot of the peak resistance change versus particle velocity data for both types of experiments. Although there is no unique calibration relation for the lateral gauges which permits conversion of that data to lateral stress, this is the primary goal of the current work and once this procedure has been established, calculation of the hydrodynamic curve and the strength of SiC in the shocked state will proceed.

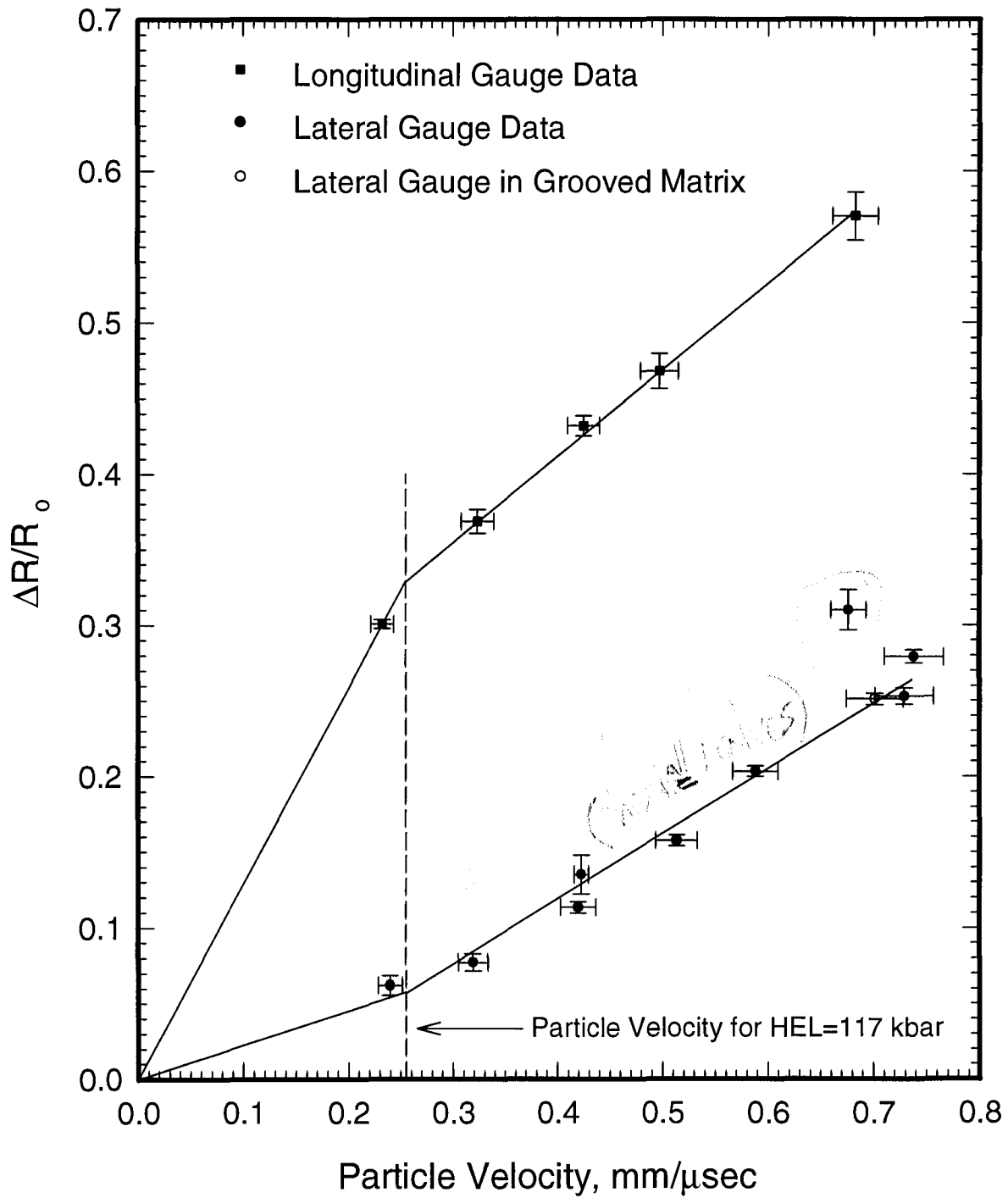


**Figure 4:** Results of all SiC piezoresistance gauge experiments. Bilinear fits are made to the upper (longitudinal gauge) data and the lower (lateral gauge) data.

## V. Error Bar Calculations

### A. Longitudinal Gauge Experiments

The error associated with the stress determination for longitudinal gauge experiments is theoretically found through a propagation of uncertainties calculation on the conversion formula:

$$\sigma_x = \frac{(\Delta R / R_o)}{K}. \quad (5.1)$$

Assuming independent and random errors in  $(\Delta R / R_o)$  and  $K$ , calculation of  $\delta\sigma_x$  would be done through:

$$\frac{\delta\sigma_x}{|\sigma_x|} = \sqrt{\left(\frac{\delta(\Delta R / R_o)}{(\Delta R / R_o)}\right)^2 + \left(\frac{\delta K}{K}\right)^2}. \quad (5.2)$$

A problem arises in the estimation of  $\delta K$ , because  $K$  is derived from a nonlinear least-squares fit of data with nonuniform uncertainties. To circumvent this problem, upper and lower calibration curves are constructed through the upper and lower uncertainty limits of the data. These curves are used along with the limiting values of  $\Delta R / R_o \pm \delta(\Delta R / R_o)$  to obtain  $\sigma_x \pm \delta\sigma_x$ . Errors in  $\Delta R / R_o$  are derived from: differences between the two gauge readings (in two-gauge shots), uncertainties in observed peak values, and errors in the initial resistances of the gauge element and gauge leads. The contribution of the last of these is minimal compared to the first two.

The equation for the copper impactor Hugoniot in  $\sigma_x - u_p$  space is taken from Feng and Gupta [3] as:

$$\sigma_x = 352.6u' + 132.1u'^2, \quad (5.3)$$

where  $u' = V_o - u_p$ . As with the stresses, a representation of  $\delta u_p$  can be obtained through propagation of uncertainties:

$$\delta u_p = \sqrt{\left(\frac{\partial u_p}{\partial V_o} \delta V_o\right)^2 + \left(\frac{\partial u_p}{\partial \sigma_x} \delta \sigma_x\right)^2}. \quad (5.4)$$

These two equations and a knowledge of  $\delta V_o$  and  $\delta \sigma_x$  can be used to calculate  $\delta u_p$ .

### B. Lateral Gauge Shots

The Hugoniot for this material is shown in Figure 3. For a given impact velocity and its uncertainty, the copper Hugoniot can be intersected with this curve in  $\sigma_x - u_p$  space to

determine  $\sigma_x \pm \delta\sigma_x$ . Equations (5.3) and (5.4) can then be used to find the corresponding  $u_p$  and  $\delta u_p$ .

## VII. Conclusions

Peak resistance changes were determined for all experiments except 94-044. In the longitudinal gauge experiments, no clear break was seen in any of the records, despite shocking the material to well above the HEL of about 120 kbar. In shot 94-019, the material was shocked to about 175 kbar and the gauge was placed 8 mm from the impact face and still no obvious two-wave structure developed. Based on the longitudinal gauge experiments and material modeling, a Hugoniot curve in  $\sigma_x - u_p$  space was constructed. Due to the nature of the wave profiles, a conversion to  $\sigma_x - \mu$  space using the jump conditions is not possible.

In the lateral gauge experiments, deviation from a square pulse is not seen at a shock stress of 130 kbar, but is seen in the second gauge record (12.7 mm depth) in an experiment where the peak stress is about 150 kbar. Above 185 kbar, clear breaks are seen in the lateral gauge records.

Since conversion of lateral gauge resistance change to lateral stress is not developed yet, conclusions on the strength of SiC in the shocked state can only be qualitative at the moment. The plot of peak resistance change versus peak particle velocity of Figure 4 clearly indicates that the shocked material retains a substantial amount of strength at least up to about 250 kbar.

## V. References

- [1] Wong, M.K. (1991), "Experiments and Analysis to Understand the Response of Lateral Piezoresistance Gauges under Dynamic Loading," Ph.D. thesis, Washington State University.
- [2] Brar, N.S. and Gupta, Y.M. (1986), "Dynamic Response of Manganin Foil Gauges to 185 kbars," SDL Internal Report Number 86-01, Washington State University.
- [3] Feng, R. and Gupta, Y.M. (1994), "Material Model for OFHC Copper for Use in Shock Wave Experiments and Calculations," SDC Internal Report Number 94-02, Washington State University.
- [4] Feng, R., Raiser, G.F. and Gupta, Y.M. (1994), "Shock Response of Silicon Carbide Undergoing Inelastic Deformation," *submitted for publication in J. Appl. Phys.*
- [5] Grady, D.E. and Crawford, D.A. (1993), "Dynamic Properties of Armor and Warhead Materials MOU FY93 Annual Report," Technical Memorandum TMDG0593, Experimental Impact Physics Department, Sandia National Laboratories.
- [6] Gupta, Y.M. and Gupta, S.C. (1987), "Incorporation of Strain Hardening in Piezoresistance Analysis: Application to Ytterbium Foils in a PMMA Matrix," *J. Appl. Phys.* 61(2), 489.

Crystal Structure	$\alpha$ -SiC (6H)
Grain Size <sup>a</sup>	4.0 $\mu$ m
Density	3214 $\pm$ 14 kg/m <sup>3</sup>
Longitudinal Wavespeed <sup>b</sup>	12.175 $\pm$ 0.085 km/sec
Shear Wavespeed <sup>b</sup>	7.735 $\pm$ 0.045 km/sec
Young's Modulus	446 GPa
Bulk Modulus	220 GPa
Shear Modulus	192 GPa
Fracture Toughness <sup>a</sup>	5.2 MPa $\sqrt$ m

<sup>a</sup>Supplier's figures

<sup>b</sup>From ARL

Table I - Summary of Material Properties



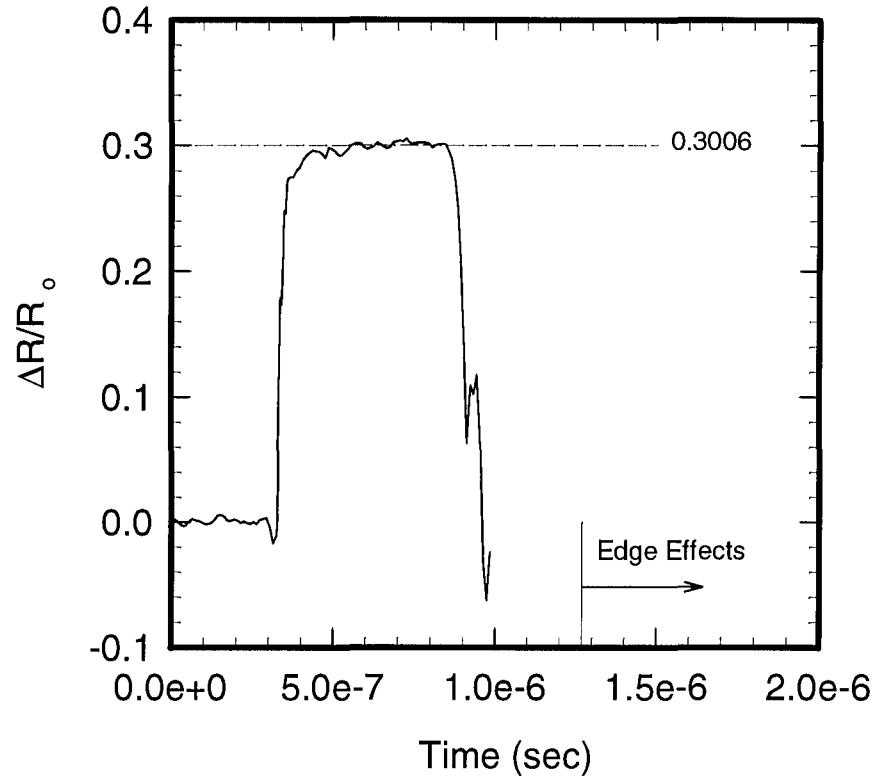
## **APPENDIX A - LONGITUDINAL GAUGE EXPERIMENTS**

### Shot 93-017

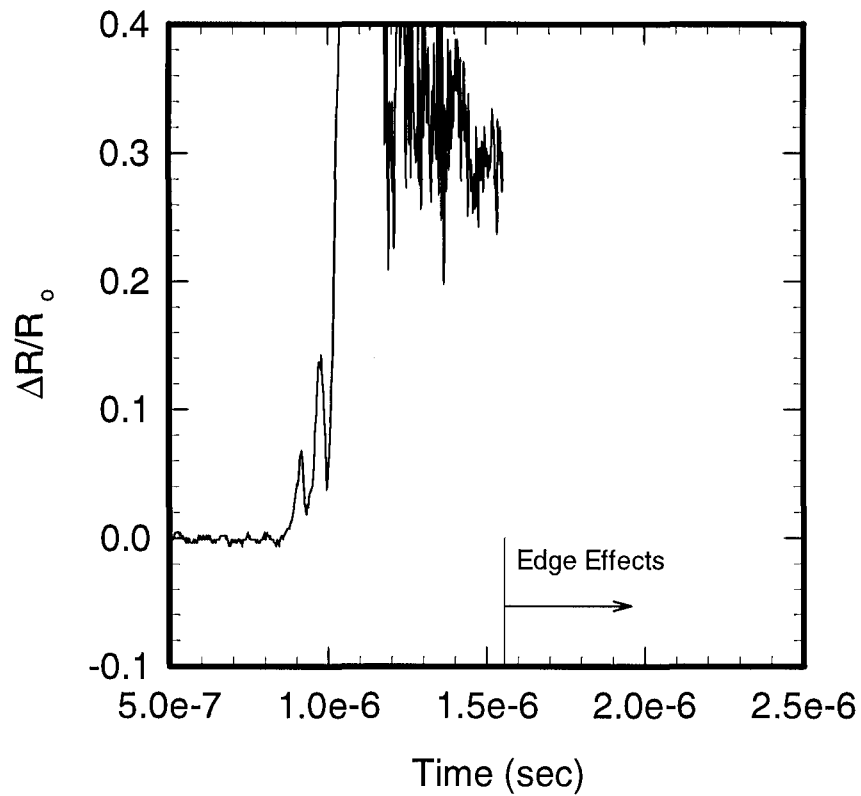
Gauge Type:	Longitudinal
Longitudinal Stress in the Matrix:	107.5 kbar
Impactor Material:	OFHC Copper
Projectile Velocity:	0.5067 mm/ $\mu$ sec
Approx. Impactor Thickness:	2.108 mm
Calculated Pulse Width:	0.932 $\mu$ sec
SiC Block Number:	2-788-3B
Gauge I Depth:	3.830 mm
Gauge II Depth:	12.001 mm
Gauge I $(\Delta R/R_o)_{peak}$ :	0.3006
Gauge II $(\Delta R/R_o)_{peak}$ :	-

Remarks: Premature failure of Gauge I (probably from the gauge breaking at the edge of the specimen) disrupted the Gauge II record. Hence, arrival times and resistance levels of Gauge II are indeterminate.

### Shot 93-017 - Gauge I



### Shot 93-017 - Gauge II

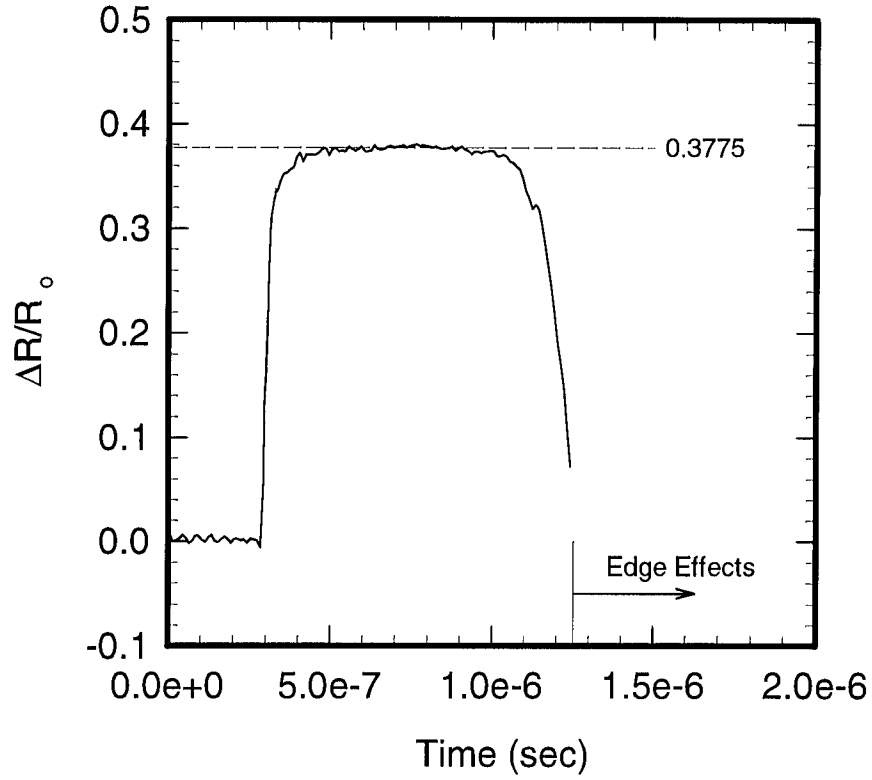


### Shot 93-052

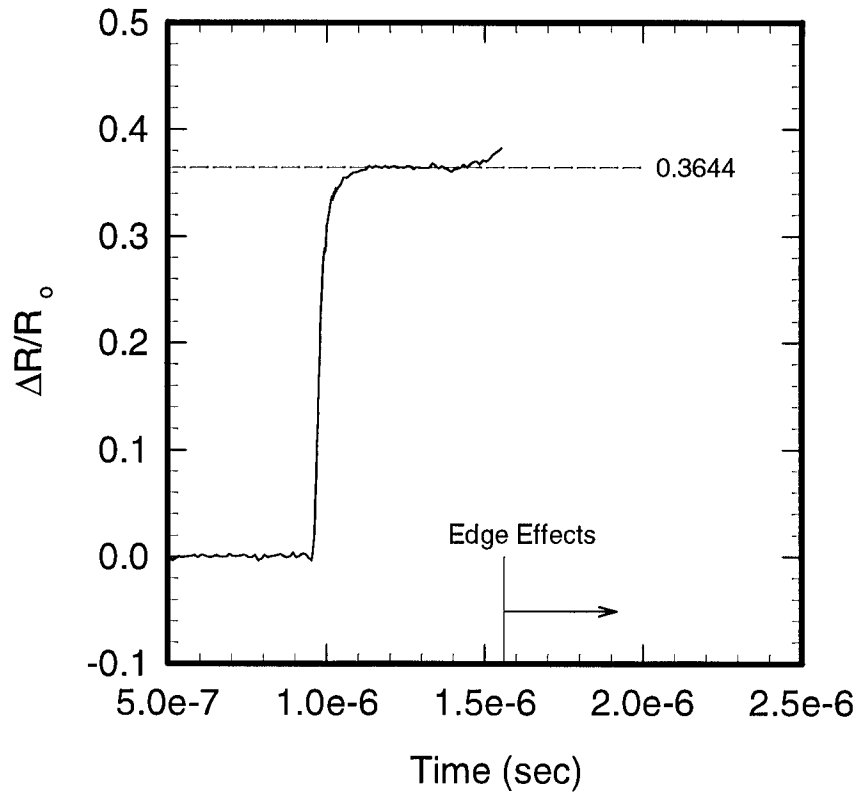
Gauge Type:	Longitudinal
Longitudinal Stress in the Matrix:	135.2 kbar
Impactor Material:	OFHC Copper
Projectile Velocity:	0.6537 mm/ $\mu$ sec
Approx. Impactor Thickness:	2.261 mm
Calculated Pulse Width:	0.967 $\mu$ sec
SiC Block Number:	2-788-3B
Gauge I Depth:	4.077 mm
Gauge II Depth:	12.263 mm
Gauge I $(\Delta R/R_o)^{peak}$ :	0.3775
Gauge II $(\Delta R/R_o)^{peak}$ :	0.3644

Remarks: Well-defined plateau regions are seen in both gauge records. Failure of Gauge I (again, probably occurring in the leads near the outer edges) occurs at the time Gauge II is at mid-plateau.

### Shot 93-052 - Gauge I



### Shot 93-052 - Gauge II

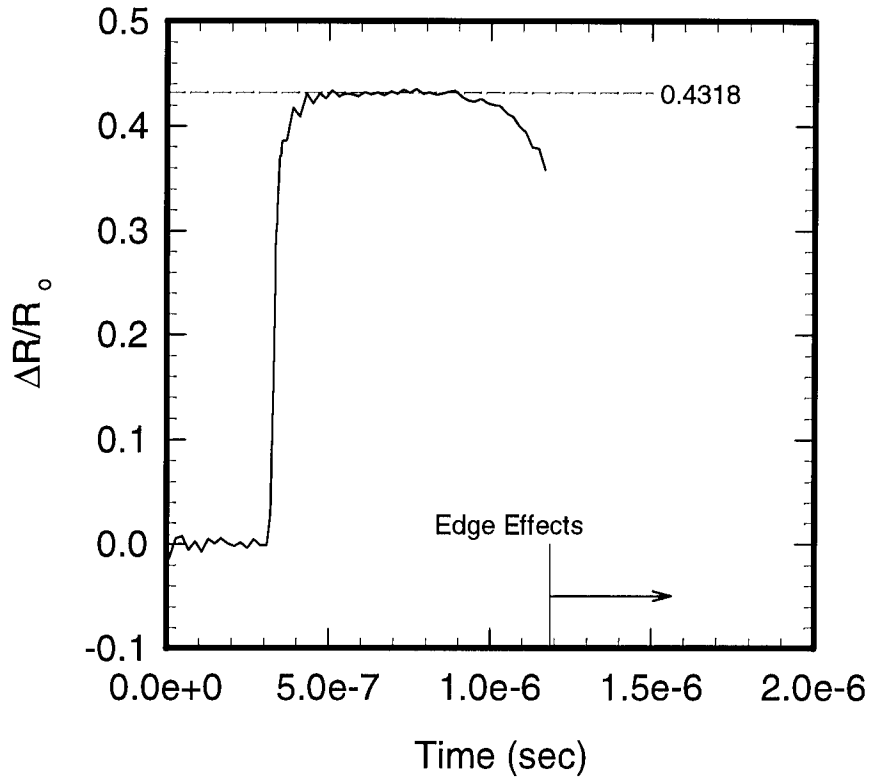


### Shot 93-063

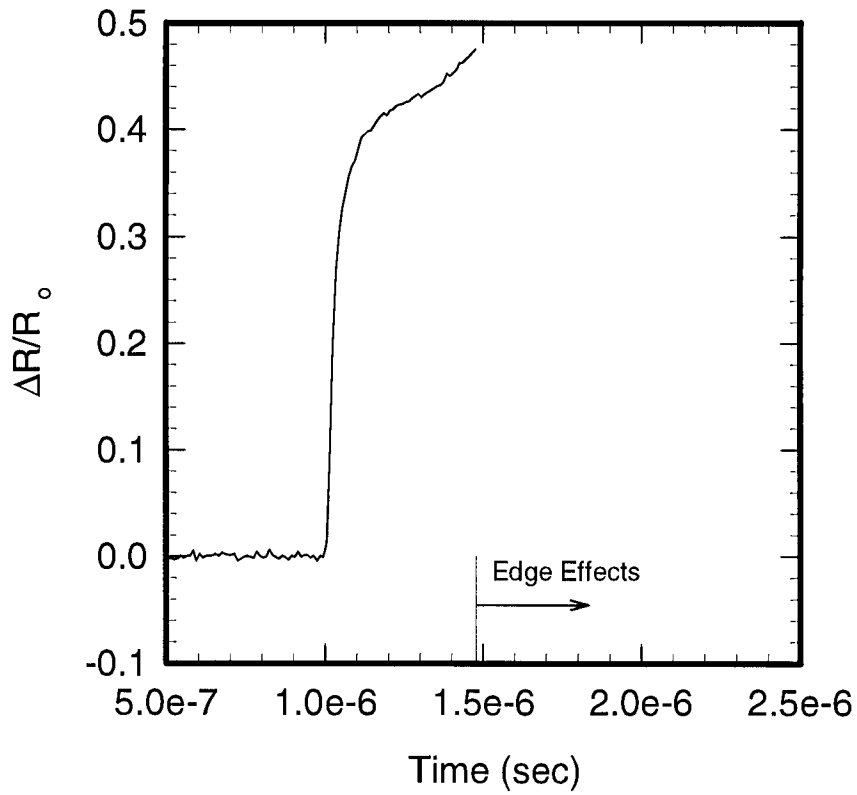
Gauge Type:	Longitudinal
Longitudinal Stress in the Matrix:	160.0 kbar
Impactor Material:	OFHC Copper
Projectile Velocity:	0.8052 mm/ $\mu$ sec
Approx. Impactor Thickness:	2.235 mm
Calculated Pulse Width:	0.926 $\mu$ sec
SiC Block Number:	2-788-3C
Gauge I Depth:	3.861 mm
Gauge II Depth:	12.154 mm
Gauge I $(\Delta R/R_o)^{peak}$ :	0.4318
Gauge II $(\Delta R/R_o)^{peak}$ :	-

Remarks: Gauge I fails as before in the other longitudinal gauge shots. Gauge I has a clear plateau, while Gauge II experiences effects from the failure of Gauge I, leaving no clear plateau to deduce.

### Shot 93-063 - Gauge I



### Shot 93-063 - Gauge II

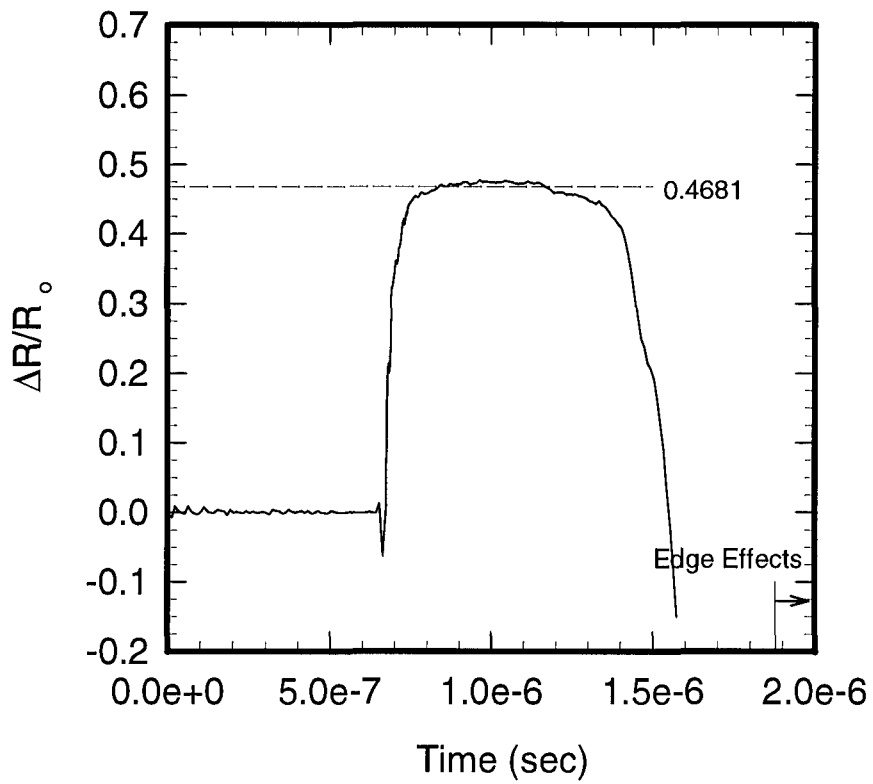


### Shot 94-019

Gauge Type:	Longitudinal
Longitudinal Stress in the Matrix:	175.3 kbar
Impactor Material:	OFHC Copper
Projectile Velocity:	0.9063 mm/ $\mu$ sec
Measured Impactor Thickness:	2.352 mm
Calculated Pulse Width:	0.955 $\mu$ sec
SiC Block Number:	4-399-2A
Gauge Depth:	8.026 mm
Gauge $(\Delta R/R_0)^{\text{peak}}$ :	0.4681

Remarks: Only one gauge is used here to minimize wave interactions between multiple interfaces. Also, specimen dimensions are chosen to delay edge effects until well after the full compressive pulse has passed the gauge. The gauge still failed prior to experiencing the full pulse; however, a good, clean plateau is seen in this record.

### Shot 94-019 - Gauge I

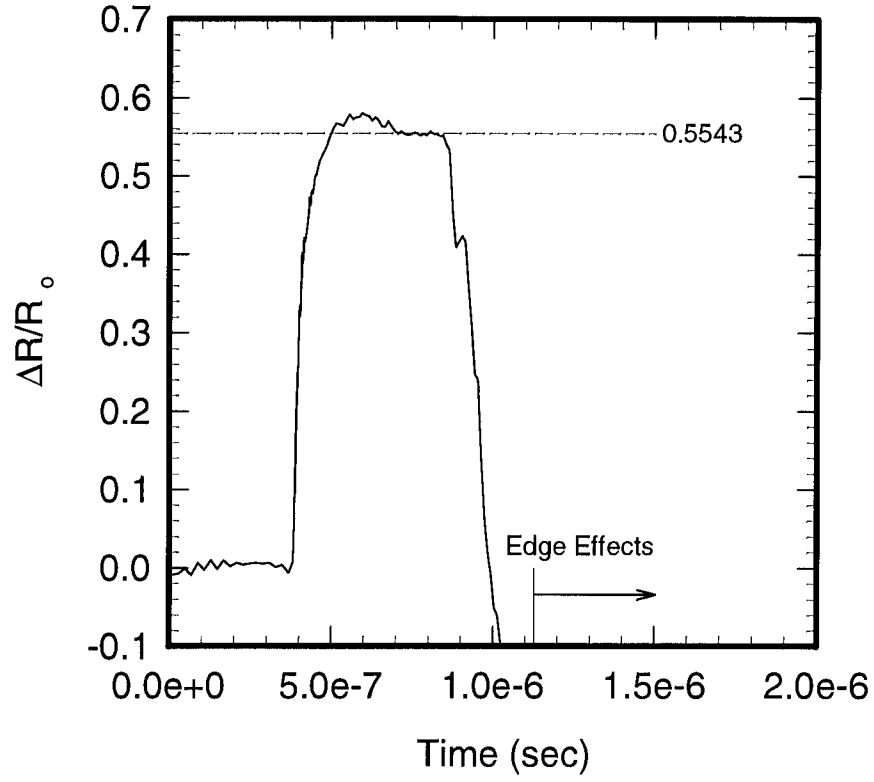


### Shot 93-073

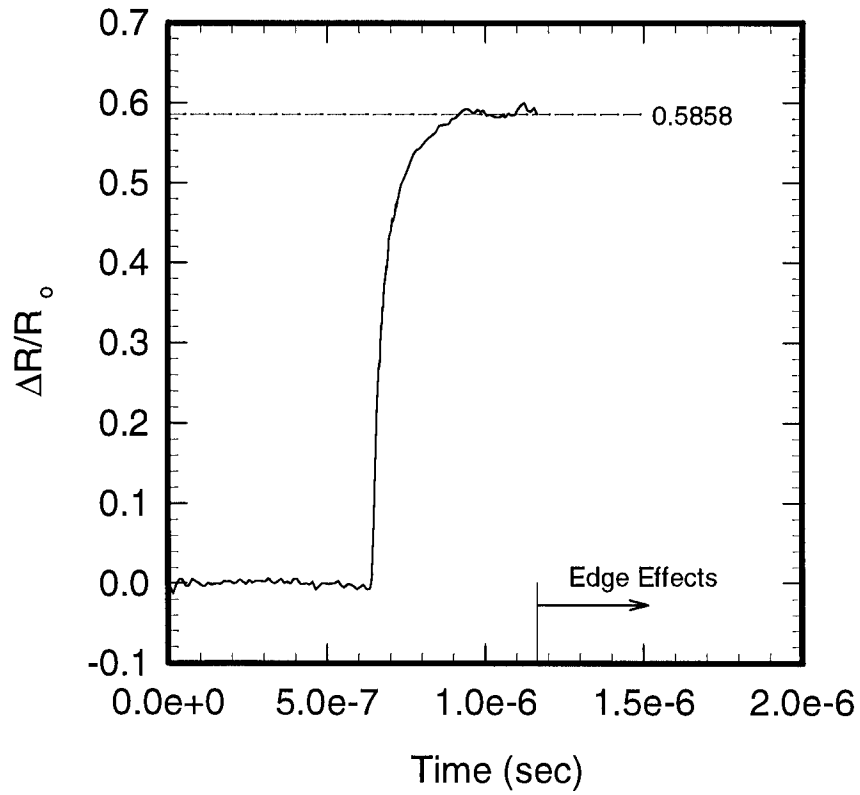
Gauge Type:	Longitudinal
Longitudinal Stress in the Matrix:	220 kbar
Impactor Material:	OFHC Copper
Projectile Velocity:	1.1682 mm/ $\mu$ sec
Approx. Impactor Thickness:	1.499 mm
Calculated Pulse Width:	0.578 $\mu$ sec
SiC Block Number:	2-788-3C
Gauge I Depth:	3.874 mm
Gauge II Depth:	6.944 mm
Gauge I $(\Delta R/R_o)^{peak}$ :	0.5543
Gauge II $(\Delta R/R_o)^{peak}$ :	0.5858

Remarks: Both gauges fail before experiencing the full pulse width. Gauge I experiences an anomalous decrease in resistance change after its peak level. This decrease is somewhat visible in the record of Gauge II also.

### Shot 93-073 - Gauge I



### Shot 93-073 - Gauge II



Experiment #	SiC Identification	Projectile Velocity (mm/ $\mu$ s)	Gauge #	Gauge Depth (mm)	$\Delta R/R_0$ (peak)	Calculated $\sigma_x$ (kbar)	Calculated Particle Velocity (mm/ $\mu$ s)
1 (93-514)	2-788-3B	0.5147	I II	4.999 13.231	0.0694 0.0709	101.1	0.2535
2 (94-005)	4-399-2A	0.5168	I II	4.230 7.201	0.0568 0.0676	101.6	0.2546
3 (93-045)	2-788-3B	0.6467	I II	4.660 12.596	0.0760 -	128.5	0.3219
4 (93-048)	2-788-3B	0.7958	I II	4.183 12.754	0.1113 0.1112	159.0	0.4027
5 (94-035)	4-399-2A	0.8002	I	8.016	0.1355	159.9	0.4051
6 (93-054)	2-788-3B	0.9336	I II	4.142 12.675	0.1559 0.1558	186.5	0.4813
7 (94-018)	4-399-2A	1.0431	I	4.080	0.2041	208	0.5463
8 (94-036)	4-399-2A	1.171	I	8.032	0.2961	232	0.6245
9† (93-070)	2-788-3C	1.2065	I II	4.228 7.051	0.2527 0.2469	239	0.6466
10 (94-044)	4-399-2D	1.211	I	7.808	-	240	0.6494
11 (93-056)	2-788-3C	1.2468	I II	4.118 12.660	0.2540 -	247	0.6717
12‡ (93-069)	2-788-3C	1.2606	I II	3.932 6.965	0.2799 -	249	0.6803

7. The most important  
 gauge was gauge #1  
 because it was the only  
 one that was able  
 to reach a plateau  
 peak levels  
 Peak levels at I level  
 are close to plateau  
 C II are close to  
 each other  
 and agreement between  
 peak levels for gauge  
 #1 and #2  
 but gauge #2  
 was not able to  
 reach a plateau  
 and gauge #3  
 was not able to  
 reach a plateau  
 single gauge data only

† Both gauges placed in grooved matrix  
 ‡ Second gauge did not reach plateau

Table III - Summary of Lateral Gauge Experiments

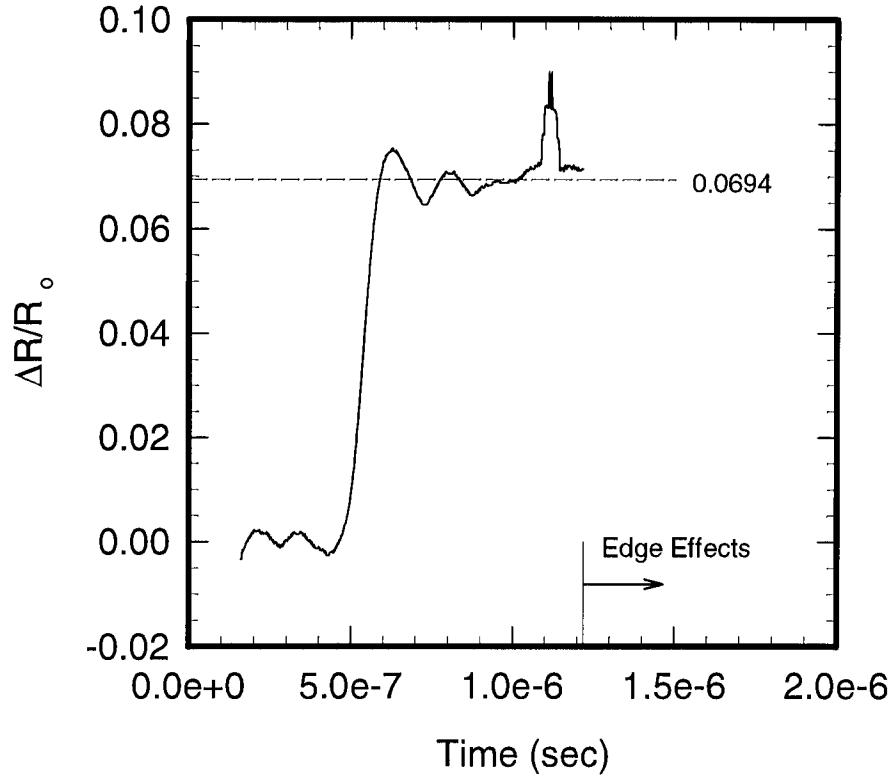
## **APPENDIX B - LATERAL GAUGE EXPERIMENTS**

### Shot 93-514

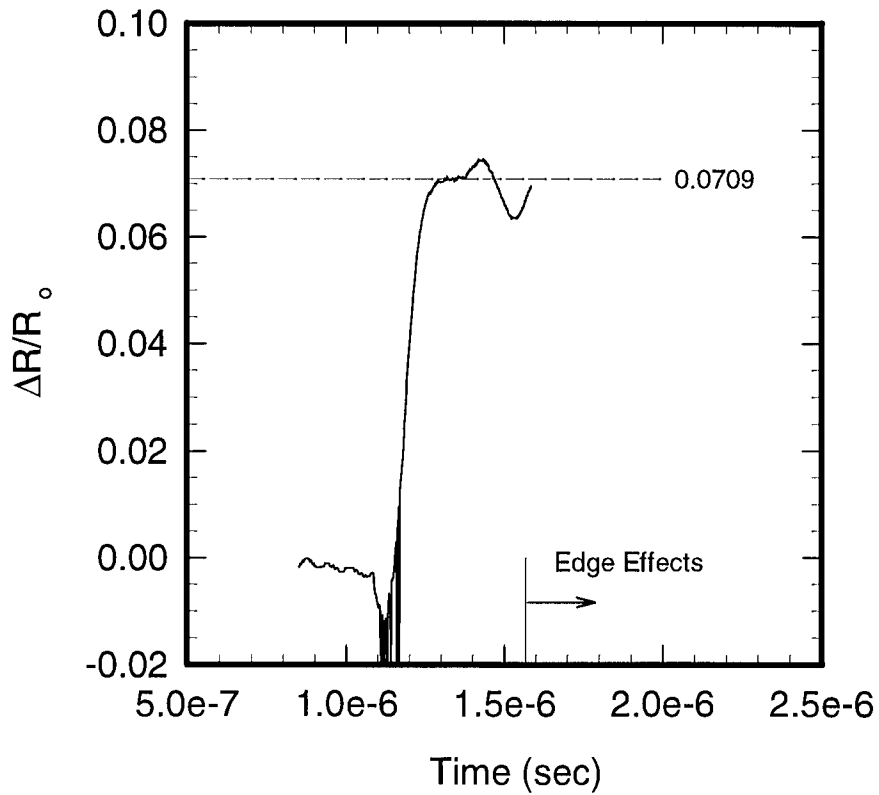
Gauge Type:	Lateral
Longitudinal Stress in the Matrix:	101.1 kbar
Impactor Material:	OFHC Copper
Projectile Velocity:	0.5147 mm/ $\mu$ sec
Approx. Impactor Thickness:	1.989 mm
Calculated Pulse Width:	0.877 $\mu$ sec
SiC Block Number:	2-788-3B
Gauge I Depth:	4.999 mm
Gauge II Depth:	13.231 mm
Gauge I $(\Delta R/R_o)^{peak}$ :	0.0694
Gauge II $(\Delta R/R_o)^{peak}$ :	0.0709

Remarks: The measurement of tilt in this shot caused a significant amount of noise in the records. This was filtered in order to present the plots shown here. The peak resistance change appears to be the same for both gauges, although there are some fluctuations near the peak level. The cause for this is probably an early unloading from the edges of the specimen.

### Shot 93-514 - Gauge I



### Shot 93-514 - Gauge II

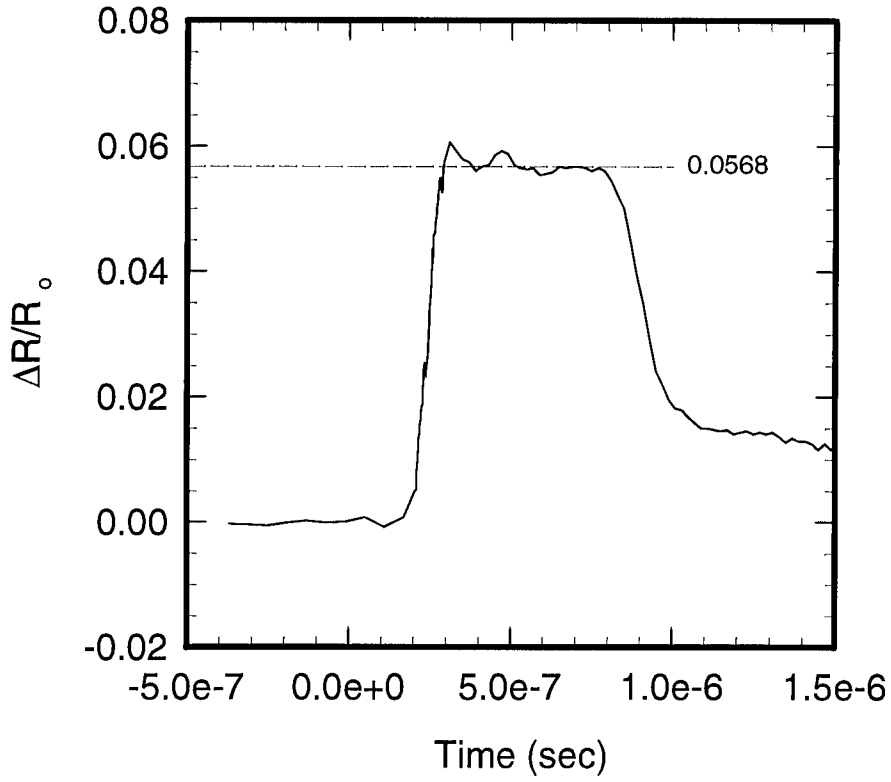


### Shot 94-005

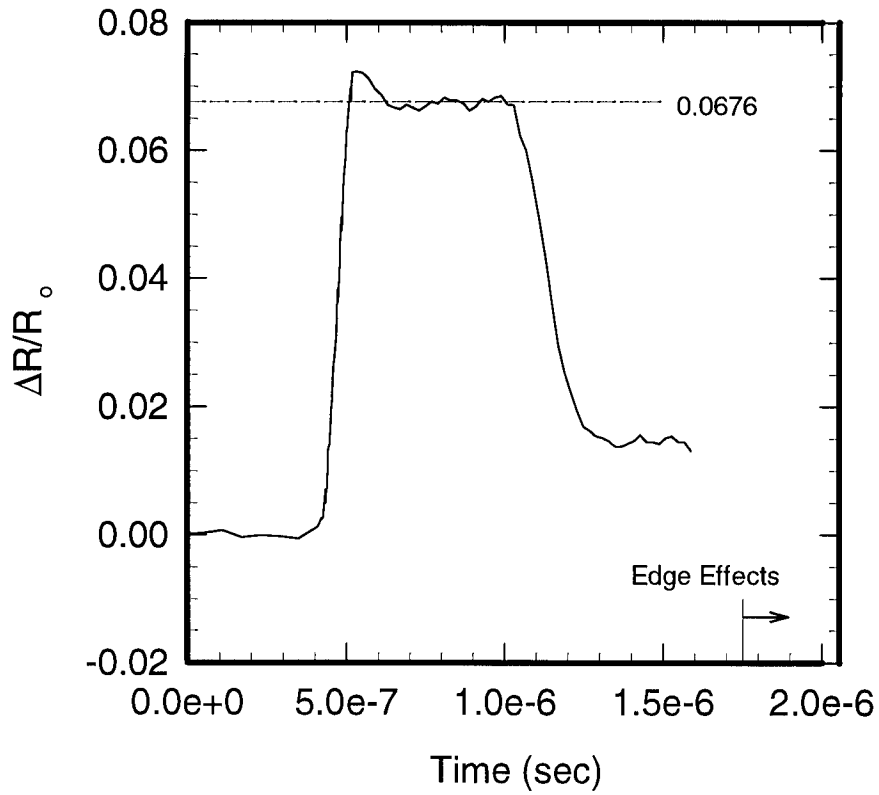
Gauge Type:	Lateral
Longitudinal Stress in the Matrix:	101.6 kbar
Impactor Material:	OFHC Copper
Projectile Velocity:	0.5168 mm/ $\mu$ sec
Measured Impactor Thickness:	1.473 mm
Calculated Pulse Width:	0.649 $\mu$ sec
SiC Block Number:	4-399-2A
Gauge I Depth:	4.230 mm
Gauge II Depth:	7.201 mm
Gauge I $(\Delta R/R_o)^{peak}$ :	0.0568
Gauge II $(\Delta R/R_o)^{peak}$ :	0.0676

Remarks: Peak resistance changes do not match very well; however, at such low values, the difference is acceptable. This shot is meant to replace SiC#1 as representative of lateral gauge response in SiC shocked below the HEL.

Shot 94-005 - Gauge I



Shot 94-005 - Gauge II

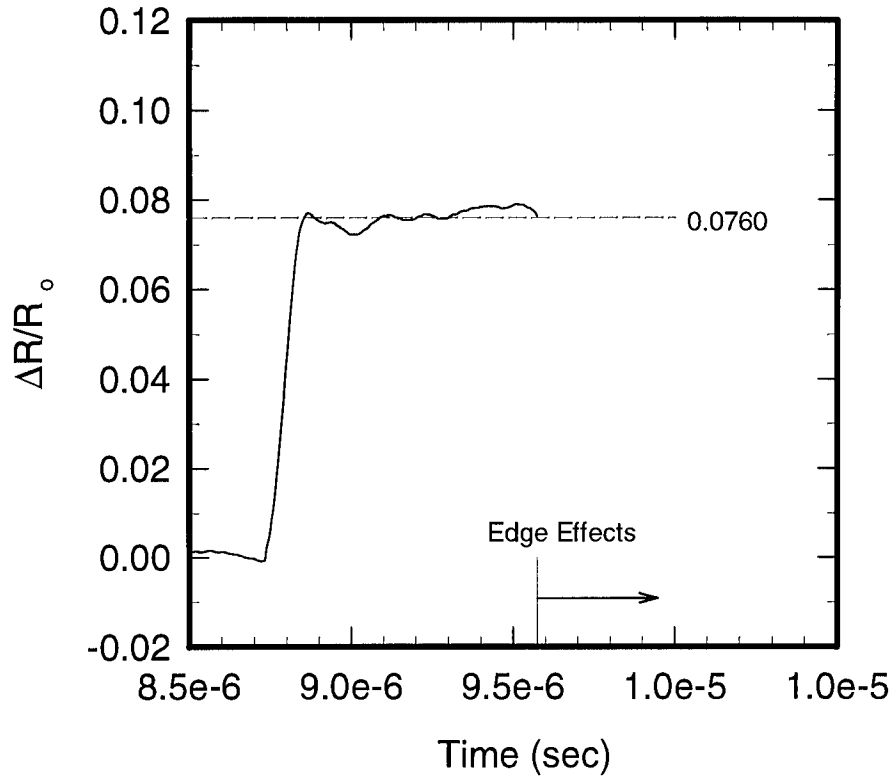


### Shot 93-045

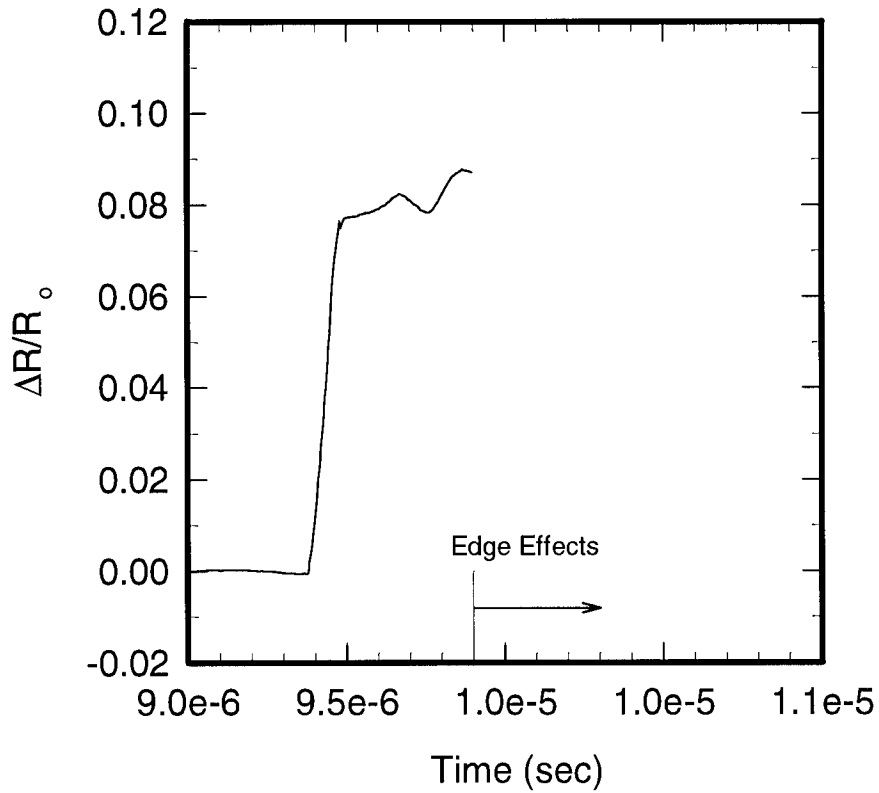
Gauge Type:	Lateral
Longitudinal Stress in the Matrix:	128.5 kbar
Impactor Material:	OFHC Copper
Projectile Velocity:	0.6467 mm/ $\mu$ sec
Approx. Impactor Thickness:	2.134 mm
Calculated Pulse Width:	0.914 $\mu$ sec
SiC Block Number:	2-788-3B
Gauge I Depth:	4.660 mm
Gauge II Depth:	12.596 mm
Gauge I $(\Delta R/R_o)^{peak}$ :	0.0760
Gauge II $(\Delta R/R_o)^{peak}$ :	-

Remarks: Peak resistance changes for both gauges match very well. Edge unloading effects are evident in Gauge II record.

### Shot 93-045 - Gauge I



### Shot 93-045 - Gauge II



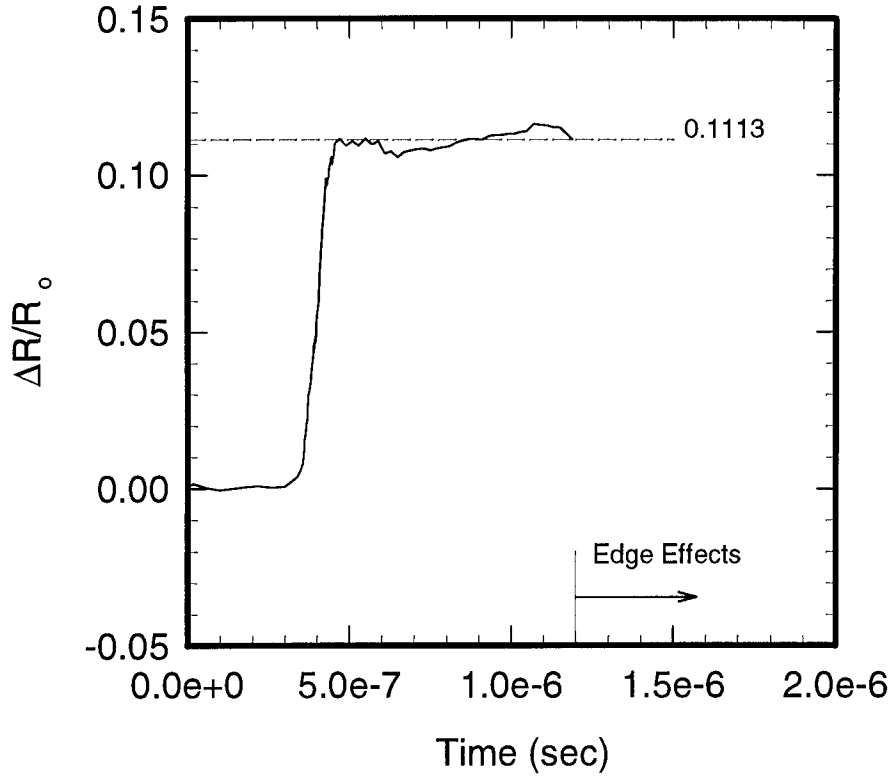
### Shot 93-048

Gauge Type:	Lateral
Longitudinal Stress in the Matrix:	159.0 kbar
Impactor Material:	OFHC Copper
Projectile Velocity:	0.7958 mm/ $\mu$ sec
Approx. Impactor Thickness:	2.032 mm
Calculated Pulse Width:	0.844 $\mu$ sec
SiC Block Number:	2-788-3B
Gauge I Depth:	4.183 mm
Gauge II Depth:	12.754 mm
Gauge I $(\Delta R/R_o)^{peak}$ :	0.1113
Gauge II $(\Delta R/R_o)^{peak}$ :	0.1112

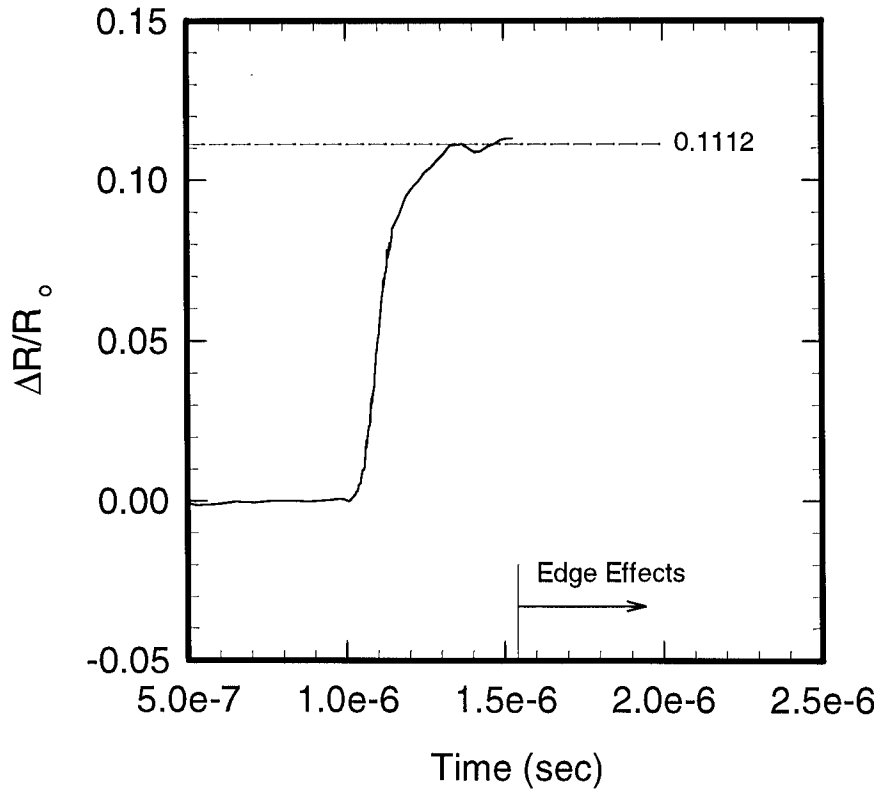
Remarks: Again, peak resistance changes match very well.

One interesting feature here is the increased risetime of Gauge II relative to Gauge I, suggesting unsteady wave propagation, at least in the lateral sense.

**Shot 93-048 - Gauge I**



**Shot 93-048 - Gauge II**

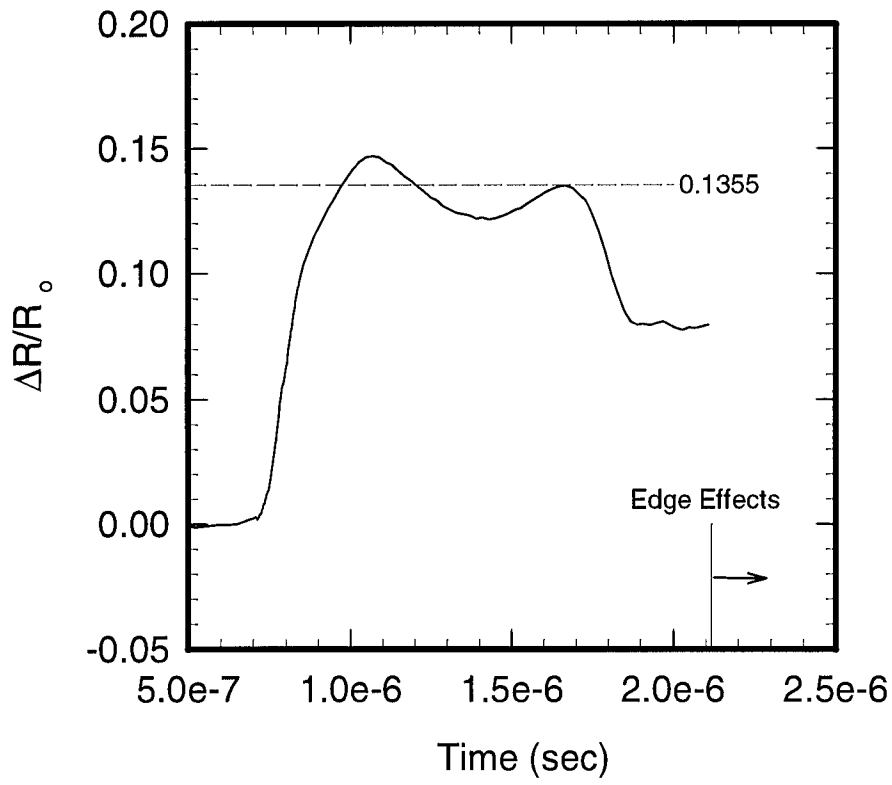


### Shot 94-035

Gauge Type:	Lateral
Longitudinal Stress in the Matrix:	159.9 kbar
Impactor Material:	OFHC Copper
Projectile Velocity:	0.8002 mm/ $\mu$ sec
Impactor Thickness:	2.446 mm
Calculated Pulse Width:	1.012 $\mu$ sec
SiC Block Number:	4-399-2A
Gauge Depth:	8.016 mm
Gauge $(\Delta R/R_0)^{\text{peak}}$ :	0.1355

Remarks: Here, the peak level is not well-defined. Appropriate error bars are necessary on this data. Reasons for the fluctuation will require further analyses/experiments.

### Shot 94-035

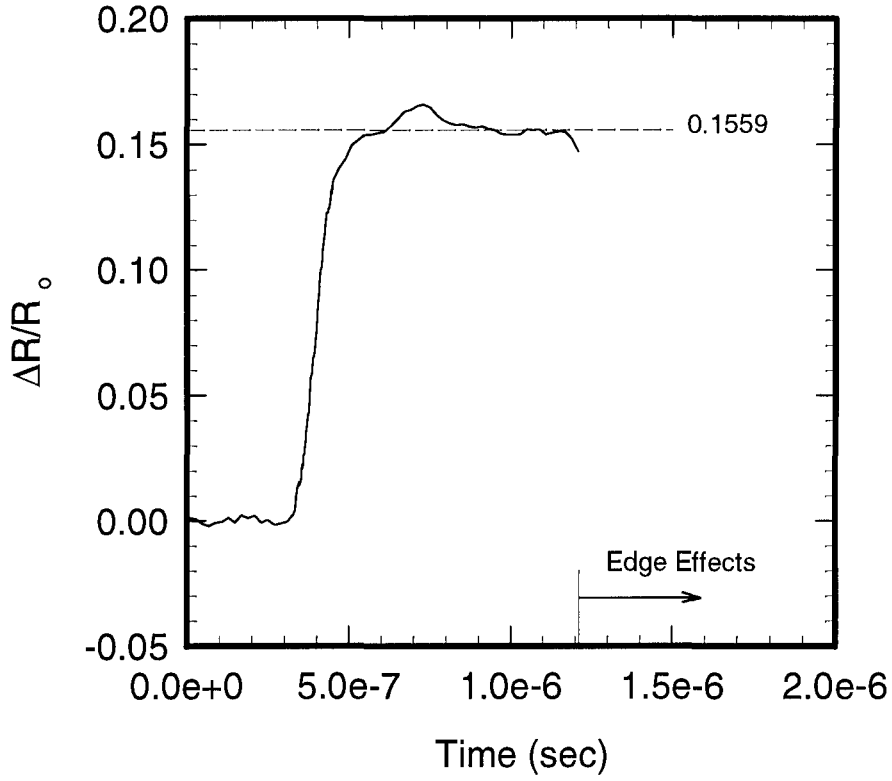


### Shot 93-054

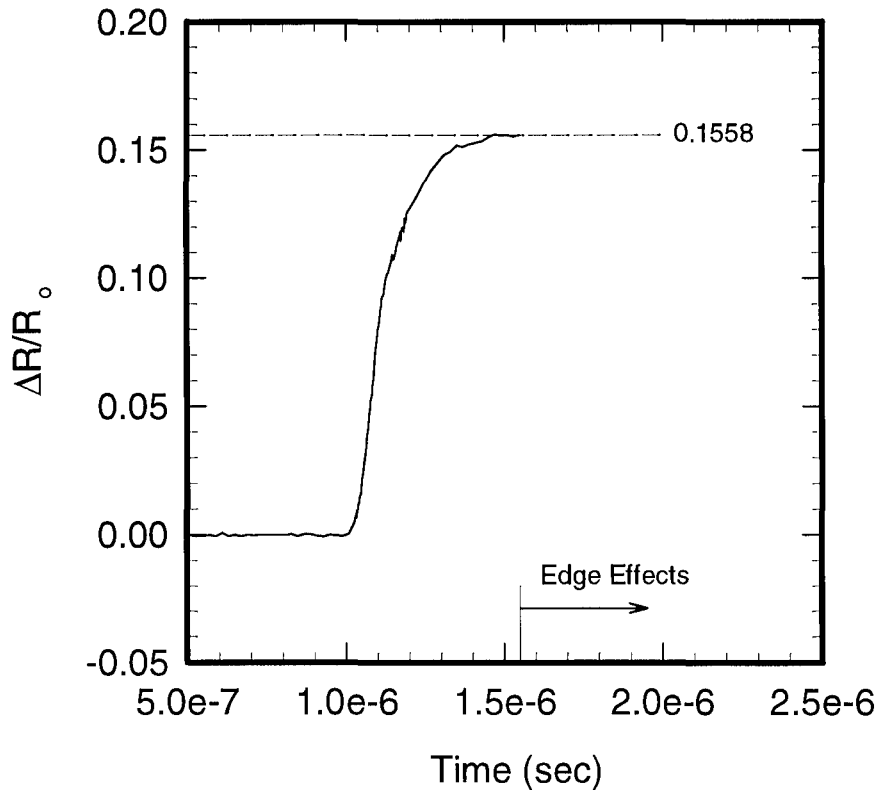
Gauge Type:	Lateral
Longitudinal Stress in the Matrix:	186.5 kbar
Impactor Material:	OFHC Copper
Projectile Velocity:	0.9336 mm/ $\mu$ sec
Approx. Impactor Thickness:	2.235 mm
Calculated Pulse Width:	0.902 $\mu$ sec
SiC Block Number:	2-788-3B
Gauge I Depth:	4.142 mm
Gauge II Depth:	12.675 mm
Gauge I $(\Delta R/R_0)^{\text{peak}}$ :	0.1559
Gauge II $(\Delta R/R_0)^{\text{peak}}$ :	0.1558

Remarks: Close agreement is observed between peak resistance changes. There is an obviously longer risetime in the second gauge record.

**Shot 93-054 - Gauge I**



**Shot 93-054 - Gauge II**

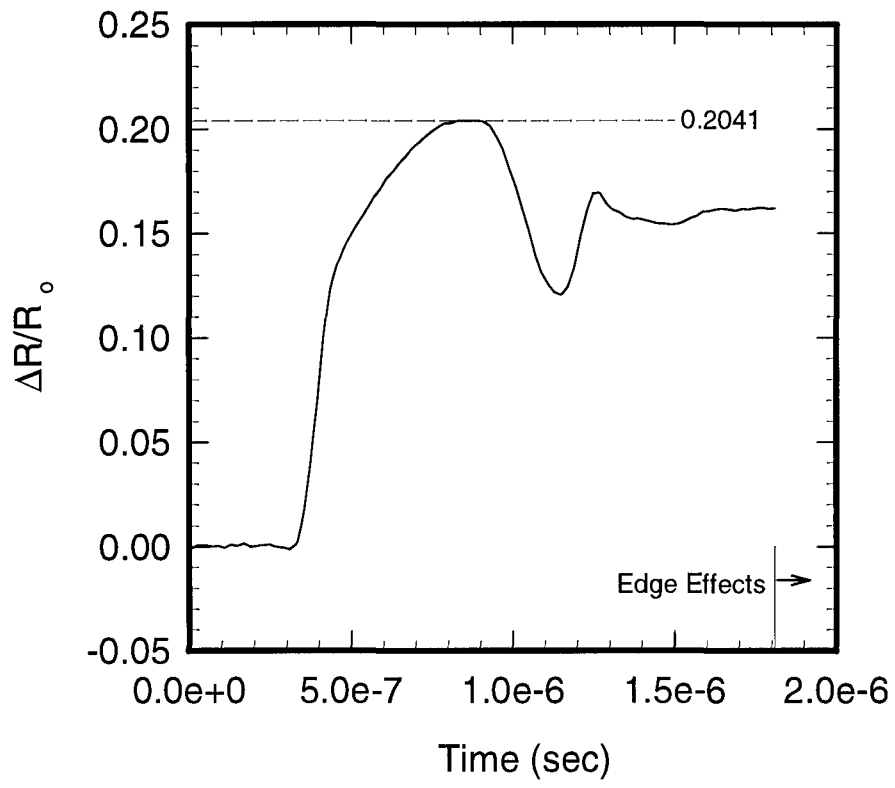


### Shot 94-018

Gauge Type:	Lateral
Longitudinal Stress in the Matrix:	208 kbar
Impactor Material:	OFHC Copper
Projectile Velocity:	1.0431 mm/ $\mu$ sec
Measured Impactor Thickness:	1.641 mm
Calculated Pulse Width:	0.648 $\mu$ sec
SiC Block Number:	4-399-2A
Gauge Depth:	4.080 mm
Gauge $(\Delta R/R_0)^{\text{peak}}$ :	0.2041

Remarks: Only one gauge is used here to minimize wave interactions between multiple interfaces. Also, specimen dimensions are chosen to delay edge effects until well after the full compressive pulse has passed the gauge. This appears to be the cleanest lateral gauge record so far. There is a clear break at about 0.13, the plateau is easily read, and a significant risetime is evident.

### Shot 94-018

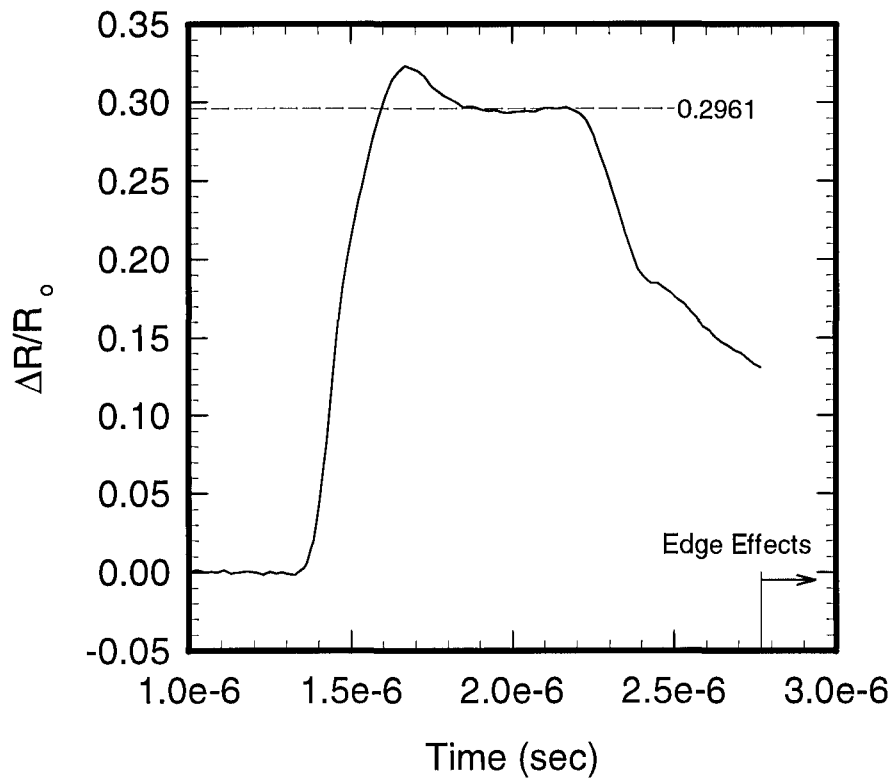


### Shot 94-036

Gauge Type:	Lateral
Longitudinal Stress in the Matrix:	232 kbar
Impactor Material:	OFHC Copper
Projectile Velocity:	1.171 mm/ $\mu$ sec
Impactor Thickness:	2.418 mm
Calculated Pulse Width:	0.925 $\mu$ sec
SiC Block Number:	4-399-2A
Gauge Depth:	8.032 mm
Gauge $(\Delta R/R_o)^{peak}$ :	0.2961

Remarks: Plateau is seen after some settling of the gauge record. Edge effects occur late and one gauge is used to minimize gauge-gauge interactions.

### Shot 94-036

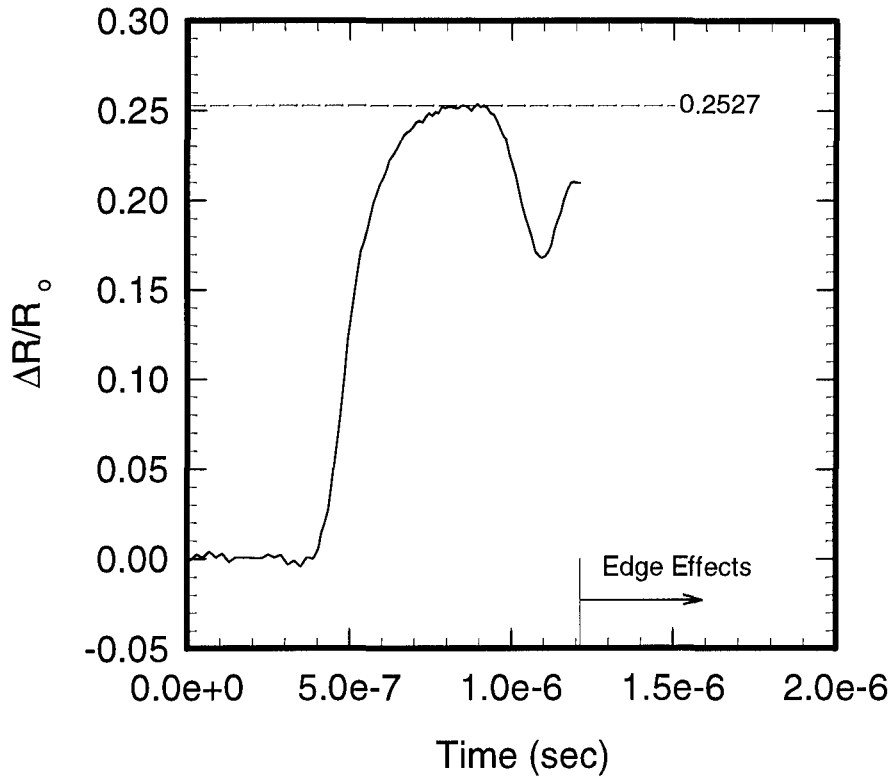


### Shot 93-070

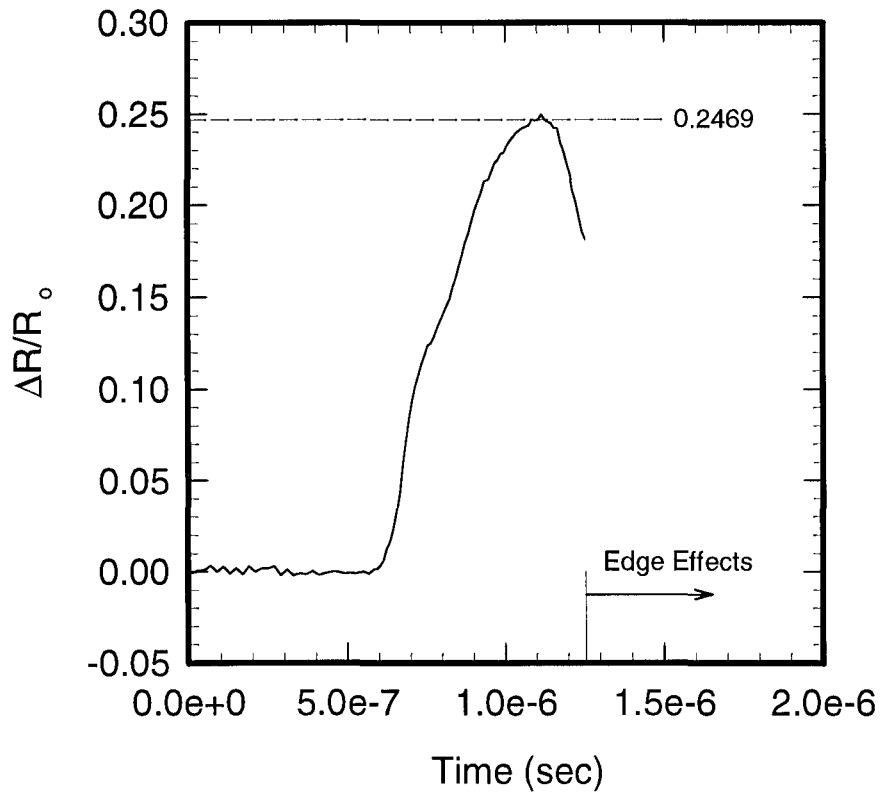
Gauge Type:	Lateral
Longitudinal Stress in the Matrix:	239 kbar
Impactor Material:	OFHC Copper
Projectile Velocity:	1.2065 mm/ $\mu$ sec
Approx. Impactor Thickness:	1.499 mm
Calculated Pulse Width:	0.573 $\mu$ sec
SiC Block Number:	2-788-3C
Gauge I Depth:	4.228 mm
Gauge II Depth:	7.051 mm
Gauge I $(\Delta R/R_0)^{\text{peak}}$ :	0.2527
Gauge II $(\Delta R/R_0)^{\text{peak}}$ :	0.2469

Remarks: In this case, gauges were placed in grooves machined into the matrix material. Gauge I has a clear plateau and since the peak in Gauge II matches closely, the peak resistance change for this shot is known with confidence.

**Shot 93-070 - Gauge I**



**Shot 93-070 - Gauge II**

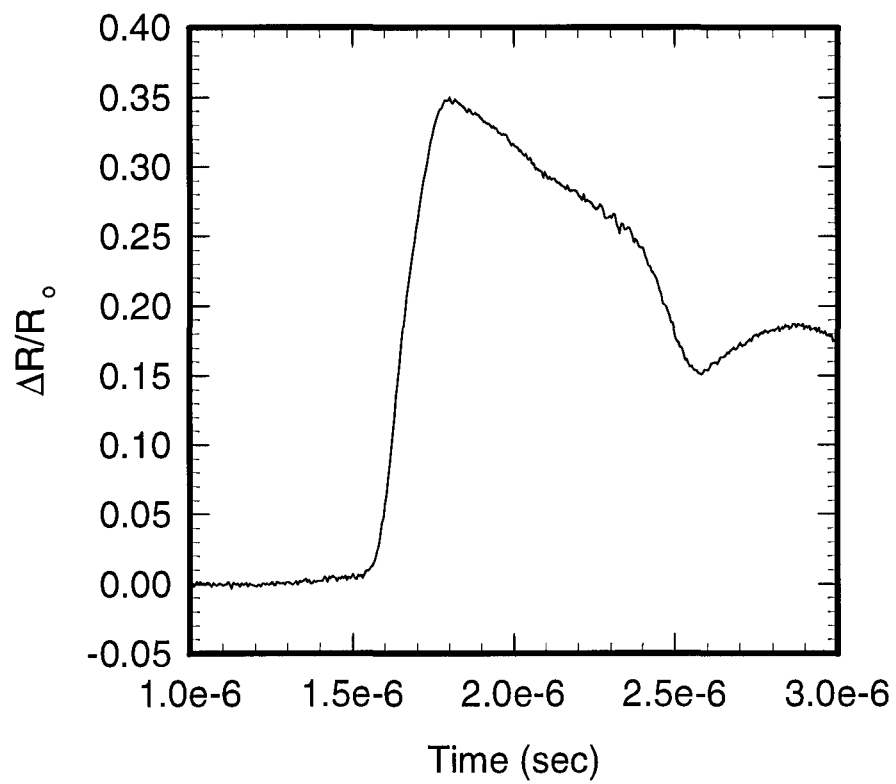


### Shot 94-044

Gauge Type:	Lateral
Longitudinal Stress in the Matrix:	240 kbar
Impactor Material:	OFHC Copper
Projectile Velocity:	1.211 mm/ $\mu$ sec
Impactor Thickness:	2.342 mm
Calculated Pulse Width:	0.889 $\mu$ sec
SiC Block Number:	4-399-2D
Gauge Depth:	7.808 mm
Gauge $(\Delta R/R_0)^{\text{peak}}$ :	-

Remarks: Peak resistance change is indeterminate. Arrival time of the signal suggests a delayed impact, probably due to some sort of failure of the projectile.

### Shot 94-044

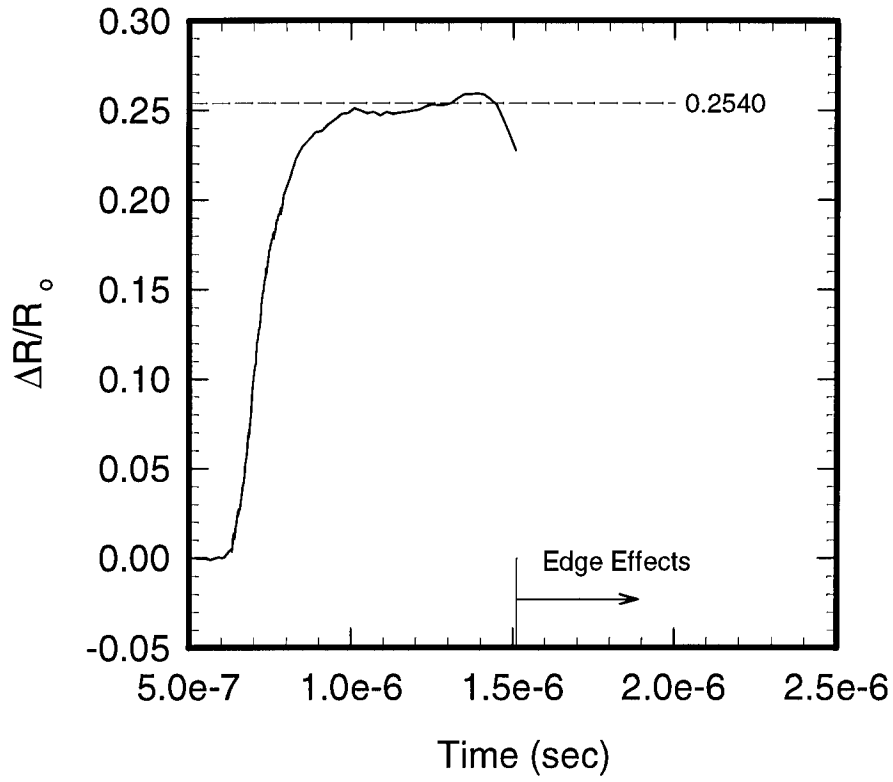


### Shot 93-056

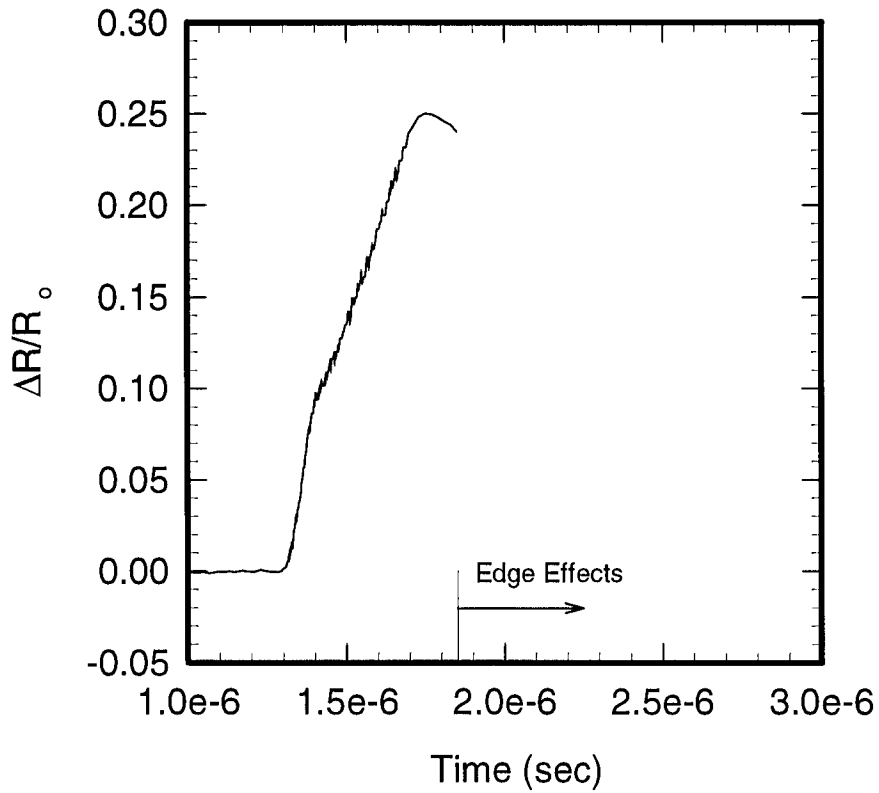
Gauge Type:	Lateral
Longitudinal Stress in the Matrix:	247 kbar
Impactor Material:	OFHC Copper
Projectile Velocity:	1.2468 mm/ $\mu$ sec
Approx. Impactor Thickness:	2.235 mm
Calculated Pulse Width:	0.848 $\mu$ sec
SiC Block Number:	2-788-3C
Gauge I Depth:	4.118 mm
Gauge II Depth:	12.660 mm
Gauge I $(\Delta R/R_o)^{peak}$ :	0.2540
Gauge II $(\Delta R/R_o)^{peak}$ :	-

Remarks: Peak resistance change for Gauge II is indeterminate as no clear plateau is reached. A longer risetime for Gauge I is observed in comparison to previous (lower stress) shots. The record of Gauge II has a significant risetime.

**Shot 93-056 - Gauge I**



**Shot 93-056 - Gauge II**

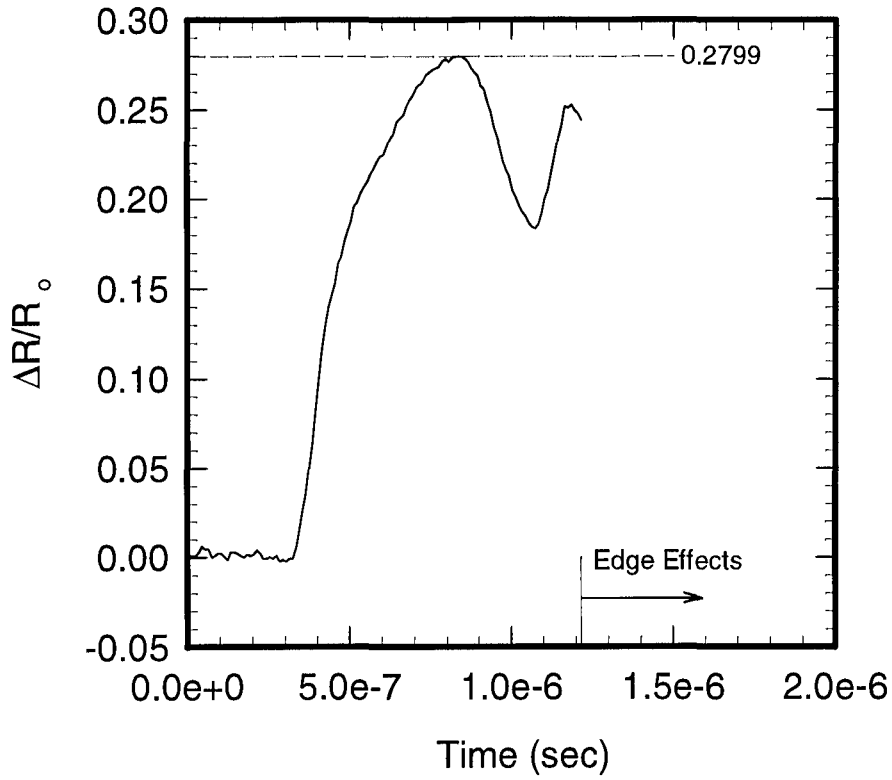


### Shot 93-069

Gauge Type:	Lateral
Longitudinal Stress in the Matrix:	249 kbar
Impactor Material:	OFHC Copper
Projectile Velocity:	1.2606 mm/ $\mu$ sec
Approx. Impactor Thickness:	1.499 mm
Calculated Pulse Width:	0.567 $\mu$ sec
SiC Block Number:	2-788-3C
Gauge I Depth:	3.932 mm
Gauge II Depth:	6.965 mm
Gauge I $(\Delta R/R_o)^{peak}$ :	0.2799
Gauge II $(\Delta R/R_o)^{peak}$ :	-

Remarks: The record for Gauge II cannot be trusted as far as the peak resistance change is concerned, since there is no clear plateau. Even Gauge I does not have a clear plateau. Both gauges experience an extremely long risetime and a "break" in slope around a resistance change of 0.10.

### Shot 93-069 - Gauge I



### Shot 93-069 - Gauge II

